

hurricane. The waves on the right side are not only generated under a higher wind but also stay under the influence of the wind field longer since they are moving with it. Therefore, the waves moving out in front of a storm are much larger than those propagating out from the rear. During the observation period, Hurricane Gloria was traveling as fast as a 150-m wave (10-second period) would propagate; thus, only waves of longer wavelengths (that is, traveling faster) would propagate ahead of the storm.

Figure 1 shows the wave pattern of the dominant waves obtained from the L-band (1.2 Ghz) imagery. Sections of the radar imagery in three different locations are also shown (Fig. 1, insets A through C). The radar imagery makes it possible to determine the waves' direction (with 180° ambiguity) and wavelength. The data obtained show several interesting features. Around the area of maximum wind, the wave direction is close to the wind direction; the wavelengths range from 100 m (behind the eye) to 275 m (at the right front of the eye). In the eye region, the waves are frequently of a long period and are short-crested (that is, have a short crest length). Away from the eye, the waves in the front half region appear to be propagating in the radial direction, which is roughly perpendicular to the local wind. They are characteristically of a long period and are long-crested (that is, have a large swell). In the rear half region, the waves are of a shorter period, and, especially in the left rear quadrant, some waves were observed propagating close to the wind direction. Possible explanations for these observations include the following: (i) the dominant waves at distances greater than 100 km from the eye are the ones that have been generated around the maximum wind region and subsequently propagated outward (7); and (ii) the radar might be less sensitive to the locally generated waves, which tend to be more chaotic than the waves generated farther away, around the eye.

Figure 1 also shows typical examples of the wave imagery. Inset A corresponds to waves near the maximum wind region, which are short-crested and appear to contain both a sea and a swell. Inset B corresponds to a region 149 km away from and ahead of the eye. The waves there are well organized and long-crested (have a swell). Inset C corresponds to a region near the center of the eye, where the crestedness of the waves is in between that of cases A and B.

We also calculated the average wave period for the four different quadrants: right front, right rear, left front, and left

rear, using the deep water dispersion relation for gravity waves. The values obtained were 11.2, 9.2, 10.9, and 9.5 seconds, respectively. These values are, on the average, larger than those reported by Pore (3) for the waves at distances greater than 130 km from the eye.

More observations are required before it will be possible to derive general conclusions on the behavior of waves around the center of a hurricane. More airborne observations are planned for 1977 and 1978, and spaceborne observations are to be made in 1978. These observations should lead to a better understanding of the statistical behavior of waves in the eye region of hurricanes.

C. ELACHI

T. W. THOMPSON*, D. KING

Jet Propulsion Laboratory, California Institute of Technology, Pasadena 91103

References and Notes

1. D. Ross, B. Au, W. Brown, J. McFadden, in *Proceedings of the Ninth International Symposium on Remote Sensing of the Environment* (Environmental Research Institute of Michigan, Ann Arbor, 1974), p. 163.
2. K. Hasselmann, D. B. Ross, P. Muller, W. Sell, *J. Phys. Oceanogr.* **G**, 200 (1976).
3. A. Pore, *Mon. Weather Rev.* **85**, 385 (1957).
4. E. G. Ward, paper OTC 2108-B, Offshore Tech-

nology Conference, Houston, Tex., 1974; R. C. Hamilton and E. G. Ward, paper OTC 2108-A, Offshore Technology Conference, Houston, Tex., 1974.

5. "Data report: Buoy observations during Hurricane Eloise, 19 September to 11 October 1975" (Environmental Sciences Division, Data Buoy Office, National Oceanic and Atmospheric Administration, Washington, D.C., 1975).
6. W. E. Brown, C. Elachi, T. W. Thompson, *J. Geophys. Res.* **81**, 2657 (1976); T. R. Larson, L. I. Moskowitz, J. W. Wright, *IEEE Trans. Antennas Propag.* **AP-24**, 393 (1976); C. Elachi, *J. Geophys. Res.* **81**, 2655 (1976); _____ and W. E. Brown, *IEEE Trans. Antennas Propag.* **AP-25**, 84 (1977); C. Elachi, *J. Boundary Layer Meteorol.*, in press.
7. I. R. Tannehill, *Mon. Weather Rev.* **64**, 231 (1936).
8. This report represents the results of one phase of research carried out at the Jet Propulsion Laboratory (JPL), California Institute of Technology, under contract NAS7-100, sponsored by the National Aeronautics and Space Administration. The Hurricane 1976 effort involved scientists from NOAA and NASA. We thank Drs. O. Shemdin (JPL) and D. Ross (NOAA, Atlantic Oceanographic and Meteorological Laboratories, Miami) for many critical and helpful comments and the personnel of NOAA (National Hurricane and Experimental Meteorology Laboratory) for providing information on Hurricane Gloria. We acknowledge the support of the NASA Earth and Ocean Dynamic Applications Program Office, the JPL Seasat Office, the Seasat Synthetic Aperture Radar team, and the Ames Airborne Science Office. We also acknowledge the courage of our colleagues E. McMillan, G. Samuelson, and T. Anderson, who volunteered to operate the radar during the flights.

* Present address: Science Applications, Inc., Pasadena, Calif. 91101.

9 May 1977; revised 23 June 1977

Slope Profiles of Cycloidal Form

Abstract. Concave profiles of basalt hills in the Darling Downs area of southeastern Queensland can be cycloidal or exponential in form. Where the complete hillslope consists of shallow soils the form is cycloidal. Where colluvial lower slopes are present the overall slope is exponential but the upper, dominantly sedentary portion is cycloidal. The cycloidal form, which corresponds to the curve of least time, appears to be associated with erosional processes and the exponential form with depositional processes.

Concave slope profiles on basalt in the Darling Downs area of southeastern Queensland extend from the edge of an upper, almost plane surface down to a lower plane surface or a local drainage line. Such concave slopes are very common throughout the world and have been described in terms of particular mathematical forms. They have been expressed as binomials (1), polynomials (2), exponential and logarithmic curves (3, 4), power curves (5), and a variety of empirical equations (6). In many of these studies the coordinates of points obtained from leveling at selected intervals have been fitted statistically to the various mathematical curves. Ruhe and Walker (4) noted that toe and foot slopes could be matched by one of their equations, but that the curve of the back slope was too steep for the same equation.

One mathematical curve with interesting properties that has been neglected

in slope analysis is the common cycloid. This curve arises as a solution to the brachistochrone problem of J. Bernoulli and is the least time path by which frictionless particles may move under gravity from one point to another not immediately beneath it. Another property is that several such particles released simultaneously anywhere on a cycloid slope will reach the lower extremity at the same time. A hillslope with such a profile would have the ideal shape for the most rapid disposal of water provided friction was not important. King (7) has attributed this property to the pediment, a landform common on the hills of the Darling Downs.

Six Darling Downs slope profiles have been tested against cycloid and exponential curves and the fits compared. The exponential curve appears to have been accepted (5) as an adequate model for many concave profiles. "True" curves of the slopes were obtained from en-

largements of photographs of the slope profiles, thus avoiding emphasis on point values as obtained with a survey traverse. The photographs were scaled by identifying significant points on these curves from large-scale contour maps (1 : 7920 with 3-m contours) and checking against the focal length of the camera. Superposition of cycloid and exponential curves on the photographs indicated that different portions of the slope profiles were approximated closely by one or the other or both of these curves. The best least-squares fit was obtained by using a nonlinear regression computer program (8) on coordinates obtained at equal horizontal intervals from the photographs.

The cycloid is best expressed as two parametric equations in polar coordinates

$$\frac{x - b}{a} = \phi - \sin \phi \quad (1)$$

$$\frac{y - c}{a} = \cos \phi - 1 \quad (2)$$

where a is the diameter of the generating circle (a scaling parameter), ϕ is the turning angle of the generating circle ($0 < \phi < \pi$ for hillslopes), x is the horizontal distance along the hillslope profile, y is the vertical height of the hillslope profile, and b and c are parameters for convenient translation of the axes.

The exponential can be expressed in a similar form

$$\frac{x - b'}{a'} = \phi \quad (3)$$

$$\frac{y - c'}{a'} = \exp(-\phi) \quad (4)$$

where a is a scaling parameter and b' and c' are translation parameters.

The results of the nonlinear regression analyses on the six hillslopes tested are summarized in Table 1. The cycloid curve gave a better fit for the Wyangapinni, Umbiram Creek, and Majuba hillslopes, whereas the exponential gave a better fit for the Dummies, Mount Gowrie, and Mount Russell hillslopes. The latter hillslopes have long extended colluvial slopes which are not present in the former. It is not valid to use a standard F test on the ratio of error mean squares because the two variances may not be independent. It may be stated that the probability of the first three slopes being closer to a cycloid and the latter three slopes being closer to an exponential is 1 in 64. Examples of the two types of hillslopes, Wyangapinni and Dummies, are shown in Figs. 1 and 2, respectively.

However, the upper portions of the

Table 1. Comparison of cycloid and exponential curves for complete slopes. Abbreviations: N , number of points; EMS, error mean square.

Hillslope	N	Vertical height (m)	Cycloid			Exponential			EMS ratio, cycloid/exponential
			a (m)	EMS (m ²)	Variance accounted for (%)	a (m)	EMS (m ²)	Variance accounted for (%)	
Wyangapinni	21	88.1	176.0	0.2864	99.97	162.3	2.0913	99.76	0.14
Umbiram Creek	11	5.2	9.84	0.0022	99.92	8.61	0.0097	99.65	0.23
Majuba	10	59.4	171.8	0.2641	99.94	136.8	1.6149	99.66	0.16
Dummies	25	134.4	313.5	19.8756	98.70	188.7	1.5875	99.90	12.52
Mount Gowrie	25	201.2	586.8	130.2662	96.46	256.3	4.3272	99.88	30.10
Mount Russell	13	54.2	147.1	7.3555	97.73	75.5	0.3145	99.90	23.39

Table 2. Comparison of cycloid and exponential curves for upper slopes. Abbreviations: N , number of points; EMS, error mean square.

Hillslope	N	Cycloid			Exponential			EMS ratio, cycloid/exponential
		a (m)	EMS (m ²)	Variance accounted for (%)	a (m)	EMS (m ²)	Variance accounted for (%)	
Dummies	15	194.3	0.9192	99.94	191.6	2.5521	98.83	0.36
Mount Gowrie	13	262.2	1.3648	99.97	251.6	6.5801	99.83	0.21
Mount Russell	6	61.8	0.3308	99.88	65.7	0.0696	99.97	4.75

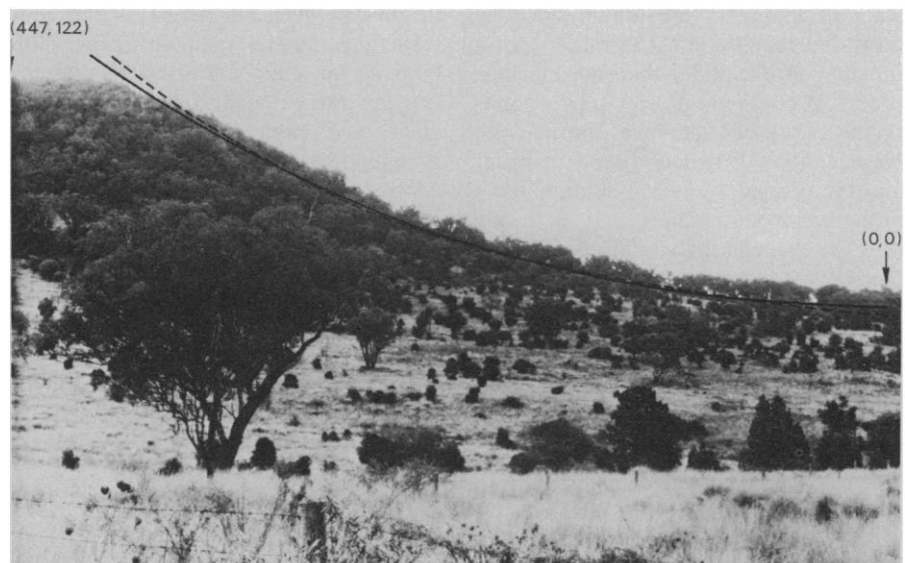


Fig. 1. Wyangapinni hillslope. (Solid curve) Best fit cycloid; (dashed curve) best fit exponential. Selected coordinates (x,y) are given in meters.

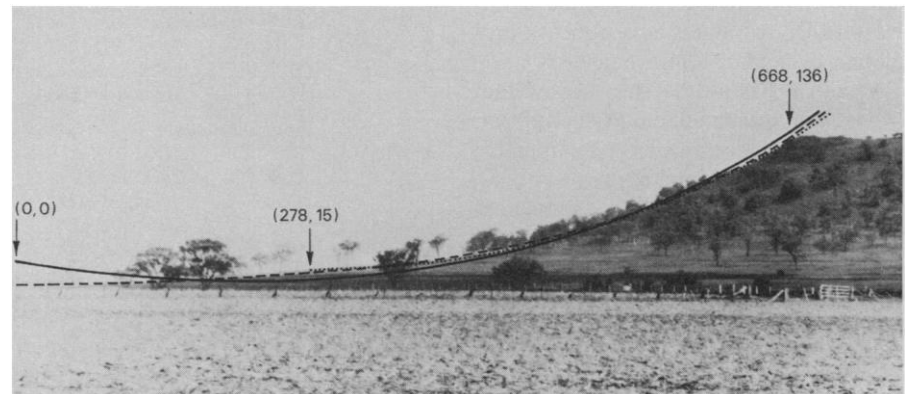


Fig. 2. Dummies hillslope. (Solid curve) Best fit cycloid; (dashed curve) best fit exponential; (dotted curve) best fit cycloid (upper slope). Selected coordinates (x,y) are given in meters.

three exponential slopes are reasonably well approximated by a cycloid. In Table 2 we use the hillslope data from the crest to the boundary between shallow, mainly sedentary soils and deeper soils on transported materials (9). These deep soils are associated with the long exponential lower slopes. No such deep soils occurred on the Wyangapinni, Umbiram Creek, and Majuba hillslopes. The Mount Russell hillslope is the only case where the exponential is better than the cycloid in Table 2, but only six points were available for curve fitting.

Taking these considerations into account, the cycloid curve appears to be a good model for hillslopes where wash processes are operating. Its "least time" shape may be the one to which erosional slopes and slopes of transportation trend, regardless of scale. Its finite limits and tangency to the vertical and horizontal axes correspond well with vertical cliffs and horizontal drainage lines. Its use may thus solve the problem raised by Ruhe and Walker (4) concerning the fit of mathematical curves on steep upper slopes.

If we assume that a hillslope tends to a state of minimum erosion in the long term and that the erosion rate is not a function of elevation, then the hillslope profile of minimum erosion corresponds to the curve of least time, the cycloid. Here contact between the wash water and the ground surface is minimized, a property recognized intuitively by King (7). The calculus of variations for ideal particle mechanics as given in Courant (10) indicates that once the cycloid is established, the erosion rate of the hillslope becomes equal at all elevations and the cycloid is maintained as erosion proceeds. Real hillslopes are subjected to frictional forces including drag and turbulence, and it would be interesting to pursue this line of analysis further.

Although the data presented here refer to southeastern Queensland, inspection has shown that some hillslopes on sandstones, shales, and granites in the southwestern United States have concave profiles of cycloidal form. Their fit is being checked. It has also been observed that Mount Mayon, an almost perfectly symmetrical volcanic cone in the Philippines, has cycloidal profiles.

On the other hand, the exponential curve seems to be a good model for hillslopes where depositional processes are operating. It obviously applies to colluvial slopes and has been observed on ash volcanoes in New Zealand.

B. J. BRIDGE, G. G. BECKMAN
CSIRO Division of Soils, Mill Road,
St. Lucia, Queensland, 4067, Australia

References and Notes

1. A. Tylor, *Geol. Mag.* **2**, 433 (1875).
2. F. C. Troeh, *Am. J. Sci.* **263**, 616 (1965).
3. G. H. Dury, *Trans. Inst. Br. Geogr.* **57**, 139 (1972).
4. R. V. Ruhe and P. H. Walker, *Trans. 9th Int. Congr. Soil Sci.* **4**, 551 (1968).
5. M. A. Carson and M. J. Kirkby, *Hillslope Form and Process* (Oxford Univ. Press, Oxford, 1972).
6. J. F. White, *Ohio J. Sci.* **66**, 592 (1966).
7. L. C. King, *Bull. Geol. Soc. Am.* **64**, 733 (1953). The pediment, a smooth landform permitting discharge in sheets over its whole area, is the natural answer to the need for rapid dispersal of storm water; it is the ideal landform to dispose of the maximum volume of water in the minimum time, with least erosional damage to the landscape.
8. P. J. Ross, *Tech. Pap. Div. Soils CSIRO Aust.* No. 6 (1971).
9. C. H. Thompson and G. G. Beckman, *Soils Land Use Ser. CSIRO Aust.* No. 28 (1959).
10. R. Courant, *Differential and Integral Calculus* (Blackie, Glasgow, 1937), vol. 2.
11. We thank G. R. Dolby, CSIRO Division of Mathematics, and P. J. Ross, CSIRO Division of Soils, for assistance with curve fitting.

17 May 1977; revised 15 August 1977

Salt-Marsh Plant Geratology

Abstract. *Measurement of individual culms of several salt-marsh plants demonstrates seasonal community change in terms of height increments and live and dead leaves. Tissue production and its ultimate transition from live to dead components and culm mortality all suggest a continuum of geratologic processes contributing to the estuarine ecosystem.*

The importance of coastal United States wetlands is becoming increasingly evident as we learn more about their contribution to estuarine and offshore ecosystems (1, 2). Primary productivity is widely used as an indicator to evaluate these wetlands; thus it is imperative that accurate estimates be made. The culm height has been suggested as the controlling parameter in determining culm biomass for many salt-marsh halophytes (3), yet the turnover of leaves from a culm, and culm mortality during the growing season, may contribute significantly to estimates of primary productiv-

ity (4). Through measurements of height increments and number of leaves, we have quantified the seasonal and spatial contribution of individual culms to overall biomass and structure of several salt-marsh plant communities.

Study sites and species were (i) Sullivan, Maine—*Spartina alterniflora* Loisel and *Spartina patens* (Aiton) Muhl.; (ii) Lewes, Delaware—*Phragmites communis* Trin., and *Spartina patens*; (iii) Sapelo Island, Georgia—*Spartina cynosuroides* (L.) Roth and *Spartina patens*. Each site represented a unique climatic regime along the eastern coast of the United States. On 5 May 1975, 50 live culms representing each species were selected at random and tagged with plastic cable ties (Ty-Rap No. TY-553M). Each culm was then measured from soil level to the tip of its tallest vegetative component to determine its height to the nearest centimeter. Live leaves, defined as any leaf having green color, were counted as well as dead leaves, having no green coloration. The three variables were monitored at 8-week intervals for each of the tagged plants during the growing season. Inspection of *Spartina patens* in Maine in May 1975 revealed dead culms; consequently, tagging of *Spartina patens* in Maine was not begun until June 1975.

We determined the change of each variable for each culm by subtracting the initial datum from the final datum of any one interval. Both positive and negative changes were computed for each interval. Algebraic summation of the changes in the numbers of live and dead leaves for a given interval resulted in a net change (ΔNet). Leaf production, senescence, abscission, and culm elongation were calculated according to Table 1. Annual leaf production is the sum of

Table 1. Calculation of tissue production, development, and death. Abbreviations: E , culm elongation; ΔH , change in height (in centimeters) of a culm during any interval; P , leaf production; ΔL , change in number of live leaves for a culm over any interval; ΔD , change in number of dead leaves for a culm over any interval; Net, $\Delta L + \Delta D$ over any interval; S , leaf senescence; and A , leaf abscission.

Value	Condition
<i>Culm elongation</i>	
$E = \Delta H$	if $\Delta H > 0$
$E = 0$	if $\Delta H \leq 0$
<i>Leaf production</i>	
$P = \Delta\text{Net}$	if $\Delta\text{Net} > \Delta L$
$P = \Delta L$	if $\Delta\text{Net} \leq \Delta L$
$P = 0$	if $\Delta L \leq 0 \geq \Delta\text{Net}$
<i>Leaf senescence</i>	
$S = \Delta D$	if $\Delta L \geq 0 \geq \Delta D$
	or if $\Delta L < 0$ and $ \Delta L \leq \Delta D$
$S = \Delta L $	if $\Delta L < 0$ and $ \Delta L \geq \Delta D$
$S = 0$	if $\Delta L \geq 0 \geq \Delta D$
<i>Leaf abscission</i>	
$A = \Delta D $	if $\Delta D < 0 \leq \Delta L$
$A = \Delta\text{Net} $	if $\Delta\text{Net} < 0$ and $\Delta L < 0$
$A = 0$	if $\Delta D \geq 0$ and $\Delta L \geq 0$